

Investigation of techniques to determine astronomical seeing conditions at Matjiesfontein

M. Nickola¹, R. Botha², W.L. Combrinck³

1. HartRAO and University of Pretoria, South Africa, marisa@hartrao.ac.za
2. HartRAO and CSIR National Laser Centre, South Africa, roelf@hartrao.ac.za
3. HartRAO, South Africa, ludwig@hartrao.ac.za

ABSTRACT

A new fundamental space geodetic observatory for South Africa has been proposed. Matjiesfontein in the Karoo has been identified as a suitable site for locating the proposed new fundamental space geodetic observatory. Lunar Laser Ranging (LLR) is one of the space geodetic techniques to be hosted on-site. LLR requires optical seeing conditions of ~ 1 arc-sec resolution level for a site to be considered suitable.

Seeing quality for various locations on the Matjiesfontein site has to be measured to determine the most suitable location for the LLR. Investigation revealed that the following are feasible techniques to determine seeing quality at the Matjiesfontein site: double star separation, Light Detection and Ranging (LiDAR) and automated seeing monitor.

Atmospheric turbulence in the boundary layer contributes significantly to the degradation of seeing quality. Atmospheric boundary-layer structure and behaviour may be simulated by a turbulence-resolving numerical model, such as the Large Eddy Simulation (LESNIC) model. The model's predictions will be compared with the quantitative seeing measurements to determine whether LESNIC is suitable for modelling seeing conditions as well as to fine-tune the model to deliver more accurate seeing predictions.

Key words: astronomical, seeing, monitor, LESNIC, LLR

INTRODUCTION

Demands for increased performance and accuracy are being placed on global geodetic networks. This has necessitated the establishment of a new fundamental space geodetic observatory in South Africa. The space geodetic observatory will host state-of-the-art equipment. It has to be located on a site suitable for optimal scientific output. (Booth and Combrinck, 2007).

The Space Geodesy Programme currently operates from Hartebeesthoek Radio Astronomy Observatory (HartRAO). HartRAO is located in close proximity to cities and industrial areas, which are sources of air and light pollution as well as Radio Frequency Interference (RFI). The need to relocate the Space Geodesy Programme to a more suitable site has become apparent, especially in view of the addition of LLR to the current suite of space geodetic equipment. LLR requires optimal optical seeing conditions. This will allow for the propagation of a laser beam through the atmosphere without excessive beam degradation. A site suitable for LLR must deliver seeing of ~ 1 arc-sec for the LLR to

achieve millimetre-level accuracy in ranging to the Moon (Combrinck et al., 2007).

A geotechnical survey has identified Matjiesfontein in the Karoo as a site suitable for the delivery of high quantity and quality geodetic data. Preliminary seeing observations were done at this site. The technique employed a small telescope to resolve features on the Moon with known angular separation. This delivered periods of good seeing (1-2 arc-sec) (Combrinck et al., 2007). Except for these preliminary seeing measurements, observations of the atmosphere over this remote site are absent. A proper characterisation of astronomical seeing conditions for various locations on-site is necessary in order to determine the most suitable on-site location for the LLR.

Seeing quality is significantly degraded by atmospheric turbulence in the boundary layer. Integration of methods from astronomical seeing and boundary layer meteorology is necessary to connect optical seeing conditions with time-space variations of atmospheric properties caused by turbulent processes (Erasmus,

1988 and 1996). Instruments currently employed for site measurements of seeing conditions, such as the Differential Image Motion Monitor (DIMM), Multi-Aperture Scintillation Sensor (MASS), Generalised Seeing Monitor (GSM) and instrumented meteorological balloons (Cherubini and Businger, 2007), to name but a few, are prohibitively expensive. Cost and availability of equipment dictated the possible methods that could be employed for determining optical seeing conditions and boundary layer meteorology at Matjiesfontein. It was decided to develop our own seeing monitor, thereby also improving in-house knowledge on the subjects of astronomical seeing and atmospheric turbulence.

The most suitable and feasible methods for studies of boundary layer meteorology consist of turbulence-resolving numerical modelling with LESNIC (Esau, 2004, Esau and Byrkjedal, 2007, and Zilitinkevich et al. 2007), atmospheric temperature profiling with LiDAR (Sivakumar, 2008) and measurement of meteorological parameters by means of a weather station. Optical seeing conditions can be determined best by implementing an automated seeing monitor on-site (Roddier, 1981) and using double star separation measurements for calibration and verification purposes (Argyle, 2004).

Data from quantitative seeing measurements will be compared with modelled results to determine whether LESNIC is suitable for modelling seeing conditions as well as to fine-tune the model to deliver more accurate seeing predictions. If a good correlation between actual seeing quality and the LESNIC model's predicted results can be found, it would be possible to employ meteorological data together with this model to select a suitable observing site. Seeing forecasts will also be made continuously.

MODELLING AND TECHNIQUES

1. LESNIC model:

The atmospheric boundary layer is described by a set of differential equations and appropriate boundary conditions. Local unstable air masses (eddies) are either resolved (large eddies) or modelled (small eddies) (Garratt, 1992).

LESNIC is based on a statistical analysis of turbulence called the Kolmogorov model of turbulence (Kolmogorov, 1941, and Tatarskii, 1961). The Kolmogorov model of turbulence provides a statistical parameter to characterise the seeing, called the Fried parameter, r_0 . It is related to the seeing, \mathcal{E}_{FWHM} , by –

$$\mathcal{E}_{FWHM} = 0.98 \frac{\lambda}{r_0} \quad (1)$$

where λ is the wavelength of observation (Fried, 1965 and 1966). A larger Fried parameter indicates better seeing conditions. The LESNIC model will be employed to deliver a prediction of the Fried parameter, r_0 .

2. Double star separation:

The light passing through a telescope's objective is diffracted. Under perfect seeing conditions a diffraction pattern, called the Airy pattern, is formed. It consists of light and dark rings surrounding a small bright Airy disc. The Airy disc represents the smallest point to which a light beam can be focused. Its diameter is directly proportional to the wavelength of the light and the focal length of the telescope but inversely proportional to the telescope aperture. The theoretical resolution limit of a telescope is given by the Rayleigh criterion –

$$\theta = 1.22 \frac{\lambda}{D} \quad (2)$$

where θ is the angular resolution, λ the wavelength of incoming light and D the telescope aperture (Argyle, 2004).

Close double stars will be observed for calibration and verification purposes. Successively closer double stars will be observed until a limit is reached where a pair can no longer be resolved. The achieved resolution limit will be compared with the telescope's theoretical resolution limit in order to determine seeing conditions.

3. LiDAR:

LiDAR is an active remote sensing technique. Laser pulses are transmitted, and backscatter from particles in the atmosphere is detected.

Assuming a Kolmogorov model of turbulence, LiDAR will be used to obtain the temperature profile of the atmosphere, $C_T^2(h)$, where h is the height above the telescope. From this, a profile of turbulence strength as a function of altitude, $C_N^2(h)$, will be obtained according to Gladstone's law –

$$C_N^2(h) = \left(80 \times 10^{-6} \frac{P(h)}{T^2(h)} \right)^2 C_T^2(h) \quad (3)$$

where P is the pressure in hPa and T the absolute temperature in K (Bean and Dutton, 1966).

The Fried parameter will be determined from the C_N^2 profile as follows –

$$r_0 = \left(16.7 \lambda^{-2} \frac{1}{\cos \gamma} \int_0^\infty C_N^2(h) dh \right)^{-3/5} \quad (4)$$

where the turbulence strength $C_N^2(h)$ varies as function of height h above telescope, γ is the zenith angle and λ the wavelength of the observed light (Roddier, 1981).

The expression for seeing thus becomes (Vernin and Muñoz-Tuñón, 1992) –

$$\mathcal{E}_{FWHM} = 0.98 \frac{\lambda}{r_0} = 5.25 \lambda \left(\int_0^\infty C_N^2(h) dh \right)^{-3/5} \quad (5)$$

4. Automated seeing monitor:

The system consists of a telescope, CCD camera and control/processing PC. Seeing varies temporally as well as spatially (Erasmus, 1988, 1996 and 2000). Stars at various positions on the night sky will be observed from various on-site locations. Numerous short exposure images of a specific source will be captured. The images will be evaluated individually, as well as stacked to obtain an average output image, the Point Spread Function (PSF). The PSF is broadened by poor seeing conditions (Roggeman and Welsh, 1996). It will be compared with the theoretical Airy function, which describes the image under ideal conditions (i.e. how the image would appear outside the Earth's atmosphere).

A quantitative measure of the seeing will be obtained by fitting a Gaussian intensity distribution to the PSF and determining the Full Width at Half Maximum (FWHM). The FWHM of a star's intensity distribution at the focus of the telescope describes the seeing, \mathcal{E}_{FWHM} . This is related to the standard deviation from the Gaussian distribution, σ , by -

$$\mathcal{E}_{FWHM} = FWHM = 2\sqrt{2 \ln 2} \sigma \approx 2.355 \sigma \quad (6)$$

according to Wargau (1994). From Equations (1) and (6) above, the Fried parameter, r_0 , will be obtained through the relation –

$$\mathcal{E}_{FWHM} \approx 2.355 \sigma = 0.98 \frac{\lambda}{r_0} \quad (7)$$

where λ is the wavelength of observation (Fried, 1965 and 1966). The Fried parameter so determined will then be compared with r_0 as predicted by the LESNIC model.

AUTOMATED SEEING MONITOR – HARDWARE CONSIDERATIONS

The optimal telescope and CCD camera combination is determined by factors such as image scale, camera pixel size and shape, as well as the required resolution. The image scale gives the amount of sky covered by a single pixel of the CCD camera. It is dependent on the CCD camera's pixel size and the focal length of the telescope. The focal length of the telescope is the effective path length light must travel through the telescope. Image scale is measured in arc-sec per pixel according to the formula:

$$\text{Image scale} = \frac{205 \times \text{CCD pixel size } (\mu\text{m})}{\text{telescope focal length (mm)}} \quad (8)$$

Smaller pixel size and longer focal length give higher resolution images (Wodaski, 2002).

Sampling refers to the number of pixels that a star image covers. With an under sampled image (too few pixels), the best possible resolution is not achieved. Critical sampling may be determined from the width of the PSF. For a Gaussian PSF, with the resolution measured across the diagonal of a square pixel, this corresponds to a critical sampling frequency of

$$FWHM = \sqrt{2} \times 2.355 = 3.33 \text{ pixels} \quad (9)$$

according to Howell (2006). In order to obtain the required resolution of 1 arc-sec, an image scale of less

$$\text{than } \frac{1 \text{ arc-sec}}{3.33 \text{ pixels}} = 0.3 \text{ arc-sec per pixel}$$

is required.

Equation (8) was used in compiling the graph depicted in Figure 1. It shows the FOV per pixel for various telescope f-ratios. A required FOV of ~ 0.3 arc-sec per pixel is achieved with telescopes within the 12" to 16" range of aperture sizes. The cost of most telescope designs within this aperture range proved to be beyond the means of our budget, with the exception of the relatively inexpensive and commercially available Schmidt-Cassegrain telescope (SCT). The computer-controlled fork mount of the SCT allows for robotic operation. The SCT operates at a focal ratio of f/10. Inserting a Barlow lens will increase the focal length of the telescope, but this adds another optical component to the light path and flaws may be magnified.

A focal ratio of f/10 limits the possible combinations of CCD camera pixel size and telescope aperture size for a FOV/pixel ~ 0.3 arc-sec to the following:

- 4.65 $\mu\text{m}/12''$, 4.65 $\mu\text{m}/14''$, 4.65 $\mu\text{m}/16''$;
- 5.4 $\mu\text{m}/14''$; 5.4 $\mu\text{m}/16''$;
- 5.6 $\mu\text{m}/14''$; 5.6 $\mu\text{m}/16''$.

Other factors to be considered for a suitable CCD camera include frame rate, dynamic range, linearity, quantum efficiency, dark current, Digital to Analogue

(D/A) resolution, signal to noise ratio (SNR) and cooling. Monochrome cameras are the preferred choice due to their higher sensitivity. Several appropriate CCD cameras (with regards to characteristics and price) are commercially available.

Seeing varies at a rate of more than 100 times a second. Frames of varying short (sub second) exposure times will therefore be captured to allow for sampling of seeing variations and short-term image wander. The images will be evaluated individually and also stacked to obtain an average output image, the PSF. Such short exposure times eliminate telescope tracking errors, precluding the need for a polar mount as well as for guiding corrections and field de-rotation.

CONCLUSIONS

Seeing is one of the most important characteristics in determining whether a site is suitable for a space geodetic observatory. Sub arc-sec seeing conditions are required for LLR in particular. It would be possible to determine seeing conditions at the Matjiesfontein site by making use of an automated seeing monitor. Measuring seeing at various locations on-site will assist in determining the most suitable location for the LLR. The LESNIC model will receive input from LiDAR and weather station measurements and will be fine-tuned, using seeing monitor data. This will be used for seeing predictions in future.

REFERENCES

- Argyle, B. (ed.), 2004, *Observing and Measuring Visual Double Stars*, Patrick Moore's Practical Astronomy Series: Springer-Verlag, London Limited, 19 & 86.
- Bean, B.R. and Dutton, E.J., 1966, *Radio meteorology: National Bureau of Standards Monograph, 92, 20*, Superintendent of Documents, US Government Printing Office, Washington.
- Booth, R. and Combrinck, W.L., 2007, *White paper towards the establishment of the International Institute for Space Geodesy and Earth Observation (IISGEO): IISGEO Draft White Paper, version 3.0, July 2007*.
- Cherubini, T. and Businger, S. (eds.), 2007, *Proceedings of the Symposium on Seeing: Kona, Hawaii, 20-22 March 2007*.
- Combrinck, W.L., Fourie, C.J.S., Croukamp, L., and Saunders, I., 2007, *Report on preliminary geotechnical and tropospheric site investigation for a proposed space geodetic observatory near Matjiesfontein in the Great Karoo: Journal of Geology, 110, 225-234*.
- Erasmus, D.A., 1988 and 1996, *Relating seeing quality to meteorological conditions: Development of seeing quality forecasts and improvement of site selection procedures: <http://www.sao.ac.za/~erasmus/overfsee.htm>*
- Erasmus, D.A., 2000, *Meteorological conditions and astronomical observing quality ('seeing') at candidate sites for the Southern African Large Telescope: South African Journal of Science, 96, 1-8*.
- Esau, I., 2004, *Simulation of Ekman boundary layers by large eddy model with dynamic mixed subfilter closure: Environmental Fluid Mechanics, 4(3), 273*.
- Esau, I. and Byrkjedal, O., 2007, *Applications of large eddy simulation database to optimization of first order closures for neutral and stably stratified boundary layers: Boundary Layer Meteorology, 125(2), 207*.
- Garratt, J.R., 1992, *The atmospheric boundary layer, Cambridge atmospheric and space science series: Cambridge University Press, 224-227*.
- Fried, D.L., 1965, *Statistics of a geometric representation of wavefront distortion: Journal of the Optical Society of America, 55(11), 1427-1435*.
- Fried, D.L., 1966, *Optical resolution through a randomly inhomogeneous medium for very long and very short exposures: Journal of the Optical Society of America, 56(10), 1372-1379*.
- Howell, S.B., 2006, *Handbook of CCD Astronomy: Cambridge University Press, London*.
- Kolmogorov, A.N., 1941, *The local structure of turbulence in incompressible viscous fluid for very large Reynolds' numbers: Comptes rendes (Doklady) de l'Academie des Sciences de l'USSR, 30, 301-305*.
- Roddier, F., 1981, *The effects of atmospheric turbulence in optical astronomy: Annual Review of Astronomy and Astrophysics, 23, 19-57*.
- Roggeman, M.C. and Welsh, B., 1996, *Imaging through turbulence: CRC Press, New York, 1*.
- Sivakumar, V., Moema, D., Bollig, C., Sharma, A., Mbatha, N., Malinga, S., Mengistu, G., Bencherif, H., and Keckhut, P., 2008, *LIDAR for atmosphere research over Africa: Laser Physics and Technology, CSIR Conference 2008*.
- Tatarskii, V.I., 1961, *Wave propagation in a turbulent medium: Dover Publications, New York*.
- Vernin, J. and Muñoz-Tuñón, C., 1992, *Optical seeing at La Palma Observatory, I. General guidelines and preliminary results at the Nordic Optical Telescope: Astronomy & Astrophysics, 257, 811-816*.
- Wargau, W.F., 1994, *Comparing seeing measurements at SAAO/Sutherland, Gamsberg/Namibia and ESO/La Silla: Monthly Notices of the Astronomical Society of Southern Africa, 53(9&10), 88*.
- Wodaski, R., 2002, *The New CCD Astronomy, How to capture the stars with a CCD camera in your own backyard: New Astronomy Press, Washington, 11-12, 166-171*.
- Zilitinkevich, S., Esau, I. and Baklanov, A., *Further comments on the equilibrium height of neutral and stable planetary boundary layers: Quarterly Journal of the Royal Meteorological Society, 133, 265*.

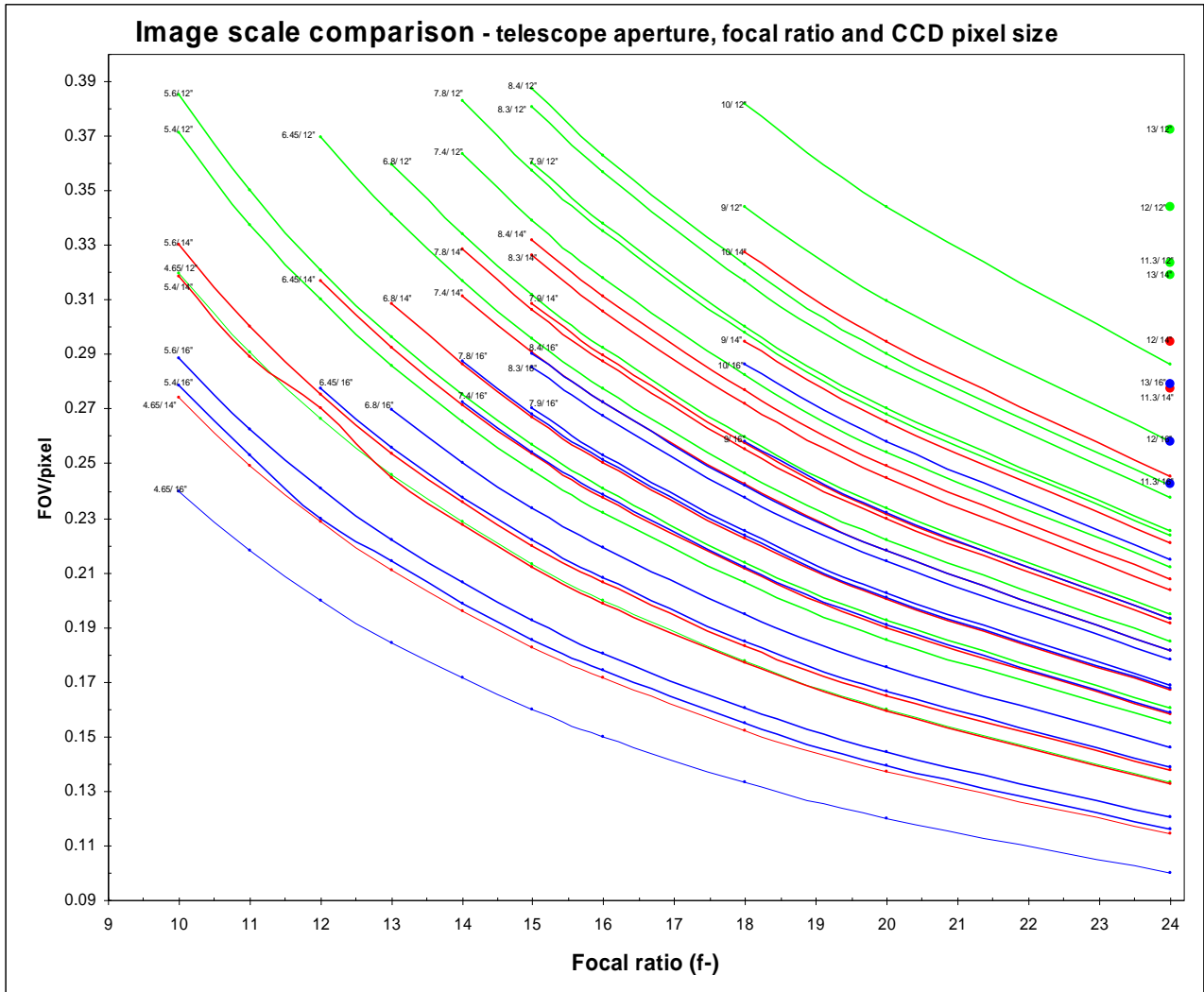


Figure 1. Graph depicting possible telescope and camera combinations. FOV/pixel in arc-sec per pixel.